CHAPTER 3

Using Satellites to Monitor Large-Scale Environmental Change: A Case Study of Cyanobacteria Blooms in the Baltic Sea

Mati Kahru

Abstract

Detection and monitoring of global and regional environmental change require extensive data sets over an extended period of time. Satellite remote sensing is among the few cost-effective means to monitor large ocean areas. Here the results of spaceborne monitoring of cyanobacteria surface blooms in the Baltic Sea are presented. Late-summer blooms of nitrogen-fixing cyanobacteria cause major environmental concern in the Baltic Sea because of their toxicity and their effects on the ecosystem through increased nitrogen input. Empirical algorithms, not dependent on exact radiometric calibration of the AVHRR imagery, were developed for the detection of cyanobacteria. A time series from 1982 to 1994 of surface cyanobacteria accumulations in the Baltic Sea was compiled by employing these algorithms. The annual cumulative area covered by the accumulations varied from 0 to over 100,000 km^2. An empirical correction procedure was proposed to better interpret time series of satellite data with varying sampling frequency. The corrected time series of cyanobacteria

Monitoring Algal Blooms: New Techniques for Detecting Large-Scale Environmental Change, edited by Mati Kahru and Christopher W. Brown.

accumulations in the Baltic did not indicate, in contrast to the commonly held perception, an increasing trend in their areal coverage during the 1982 to 1994 period. It did, however, show an El Niño-like cycle.

Introduction

In the Baltic Sea, the nitrogen-fixing cyanobacteria bloom that occurs in late summer, significantly affects the annual carbon and nutrient cycles with its increased primary production and particulate concentration.[1,2] Cyanobacteria use dissolved molecular N_2 as an additional nitrogen source which allows them to bloom in the summer when the growth of other phytoplankton is normally limited by nitrogen. During the relatively short bloom period, a significant amount of biomass is produced and potentially exported from the pelagic system.[3] Blooms of filamentous cyanobacteria in the Baltic Sea are of major environmental concern because of their toxicity and fertilizing effect on the ecosystem through nitrogen fixation.

More than two decades ago it was suggested[4] that the extent and intensity of the cyanobacteria blooms in the Baltic was increasing due to anthropogenic eutrophication. This perception among scientists and environmentalists has become more prevalent during recent years and is promoted by the established increase in nutrient loadings,[5] recent, visually impressive satellite images,[6] and results from analysis of satellite data.[7] Long-term changes in the extent of cyanobacteria blooms are hard to prove using data from conventional monitoring programs, such as shipboard sampling, due to their high spatial and temporal variability, and scarcity of data from the open sea. While the Baltic Sea is relatively small compared to the World Ocean, its area (210,000 km² for the Baltic Proper, over 400,000 km² including the gulfs, straits and Kattegat) still overwhelms conventional shipboard monitoring. Sampling is further complicated by the highly heterogeneous nature of its waters. Cyanobacteria blooms may be detected in visible satellite imagery, which provides the synoptic and repeated coverage appropriate to address this question.

The presence of cyanobacteria accumulations near the sea surface increases absorption of solar radiation in the top few meters and therefore increases the stratification and sea surface temperature.[8] The increased stratification, surface temperature and irradiance can have positive feedback on the cyanobacteria by further enhancing their buoyancy and trapping them at the top of the water column.

Satellite detection of cyanobacteria is possible due to the formation of dense accumulations near the sea surface. The surface-visible cyanobacteria blooms in the open Baltic Sea are almost always dominated by *Nodularia spumigena* whereas other species may bloom in the coastal areas.[3] In the later stages of a bloom, the filaments become positively buoyant and aggregate into large agglomerates in the surface layer, giving the impression of yellow snowflakes. The filaments are highly reflective at visible and near-infrared wavelengths due to the refractive index of the gas vesicles. At low wind speeds, the agglomerates accumulate in the top few meters to the extent that they can be observed with relatively insensitive, broad-band, space-borne instruments such as the Advanced Very High Resolution Radiometer (AVHRR). The surface accumulations form characteristic patterns due to the convergence and divergence zones of the surface current field (Fig. 3.1). These characteristic patterns are visually distinguishable from other phenomena in uncalibrated imagery without sophisticated optical models. The characteristics of cyanobacteria accumulations allow us to use both archived and current imagery from various sensors to assess the area covered by the accumulations and to detect long-term trends.

While obtaining a 20-year time series of phytoplankton biomass from ocean color data is a goal set by NASA for the future,[9] the dynamics of cyanobacteria blooms in the Baltic over two decades can be obtained now based on data from several past and present sensors possessing visible and near infrared bands, such as AVHRR, the Coastal Zone Color Scanner (CZCS), the Landsat Multi Spectral Scanner (MSS) and Thematic Mapper (TM). Imagery from terrestrial designed sensors, such as Landsat MSS and TM has shown cyanobacteria accumulations in high resolution

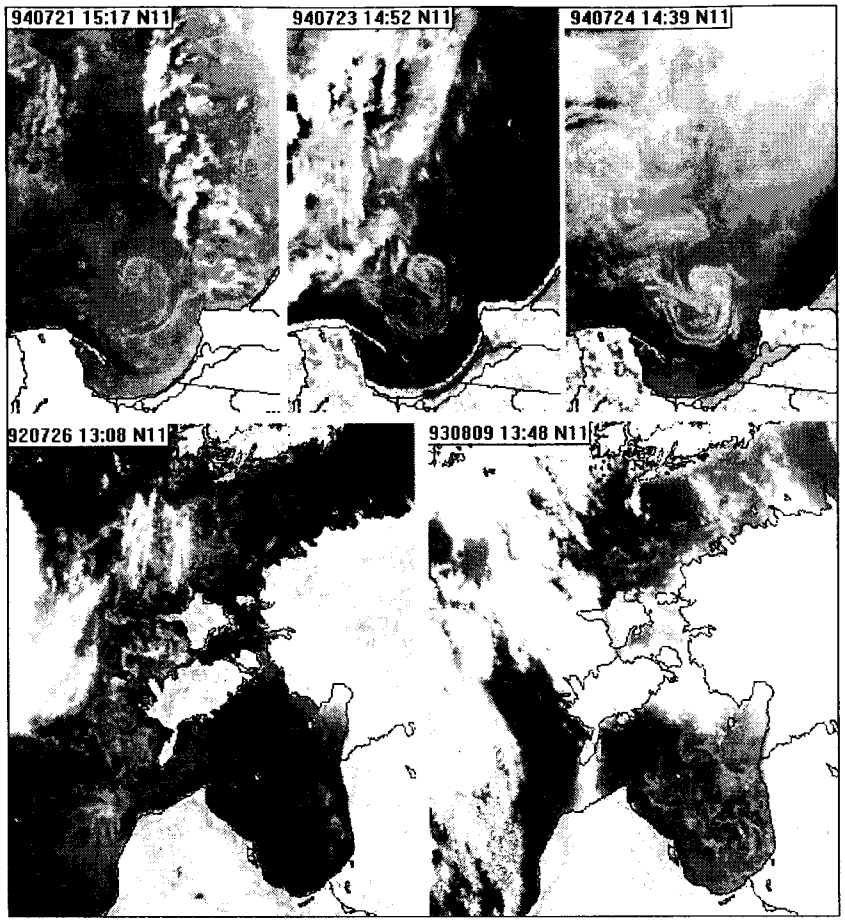

Fig. 3.1. Examples of cyanobacteria accumulations visible in NOAA-11 AVHRR band 1 images. Land and clouds are white, clear water surface is black, and cyanobacteria accumulations can be seen as curvy filaments with lighter shades of gray. The top panel shows the accumulations being advected by an eddy vortex in the Bay of Gdansk over a sequence of three images. The lower panel shows the accumulations in the Gulf of Riga (lower right) and northeastern Baltic Proper on representative images of 1992 and 1993.

since 1975,[4] yet has narrow swath width, low sampling frequency and is usually expensive. For estimating phytoplankton concentrations in the water, a specialized and highly sensitive ocean color sensor, such as the CZCS is required. Unfortunately, the CZCS operated on a limited basis between 1979 and 1986, nominally for only two hours per day.[10] Due to its irregular duty schedule and limited life span, CZCS data alone do not provide a decadal-scale time series. Dedicated ocean color sensors of this caliber, such as the Ocean Color and Temperature Scanner (OCTS) on the Advanced Earth Observing Satellite (ADEOS) will provide ocean color data in the near future.

Data from AVHRR instruments onboard NOAA polar orbiting platforms[11] provide the best coverage for retrospective analysis since 1979. The AVHRR is especially suitable for monitoring purposes due to its wide swath width (over 2000 km), frequent coverage (up to several passes per day), and availability over a long period of time. Compared to specialized ocean color sensors, the AVHRR possesses only two broadband spectral channels in the visible and near infrared, limiting spectral algorithms to distinguish cyanobacteria accumulations from certain types of clouds, suspended sediments, and bottom reflection. In spite of these technical limitations, AVHRR data can provide valuable ecological insights.

Results based on a 12-year time series of satellite-detected cyanobacteria accumulations in the Baltic[7] appeared to support an overall increase in the total area covered by cyanobacteria blooms. In a subsequent paper,[12] a correction factor was introduced to compensate for the effects of significantly higher sampling frequency during more recent years. Here, the analysis is extended to 13 years and the methods are described in greater detail.

Methods

For a time series that spans over a decade and uses several instruments with their degrading sensitivities, the exact radiometric calibrations of the various sensors becomes an important issue for intercalibration and interpretation of the results. The

calibration of visible sensors that do not have an onboard calibration capability, such as the AVHRR, has been a problem for many applications.[13] For example, even with the best available calibration coefficients, performing atmospheric correction of data from the different AVHRR instruments can result in impossible negative values of water-leaving radiances.[14] Consequently, algorithms that can be adjusted to accommodate the characteristics of individual sensors were developed.

A supervised classification algorithm to detect cyanobacteria accumulations was developed[7] and applied to NOAA-6 to NOAA-12 AVHRR data of the Baltic Sea collected from 1982 to 1994. A similar algorithm developed for CZCS is potentially more accurate due to higher sensitivity of the CZCS but has not yet been applied to larger data sets. The AVHRR empirically based algorithm relies on multiple thresholding and differences in visible, near infrared and thermal channels to distinguish cyanobacteria blooms from other common conditions (Fig. 3.2). Both the increased reflectance and a measure of spatial texture in the AVHRR visible band 1 (0.58-0.68 μm) were employed. Cyanobacteria accumulations possessed an albedo varying between 2.3% and 4%, whereas lower and higher values were designated as water and clouds, respectively. Spatial texture was calculated in 3 x 3 pixel windows. Areas with a spatial texture, measured as the variance in 3 x 3 pixel window, exceeding a certain adjustable threshold, were considered cyanobacteria blooms. Data in the near infrared band 2 (0.72-1.10 μm) and the two thermal infrared bands, 4 (10.4-11.0 μm) and 5 (11.6-12.2 μm), were used to screen clouds, haze, land and error pixels. For the AVHRR with only one thermal infrared band the channel 4-channel 5 difference test was skipped. Pixels with band 2 albedo exceeding the corresponding band 1 albedo by 0.2% albedo values were classified as land or considered an error. Pixels with the band 4 temperature colder than a seasonally varying threshold and with a band 4 and band 5 difference greater than 2°C were designated clouds. Finally, visual inspection and editing was used to eliminate pixels erroneously marked as accumulations due to variable clouds and sediment-rich coastal areas. As cyanobacteria accumulations are usually

present in the same location for more than one day, but clouds and other atmospheric effects are more transient, sequences of images were checked for consistency of the detected accumulations over several images and suspected classification errors were manually deleted.

Individual maps of cyanobacteria accumulations were composited for weekly, monthly, and yearly periods by selecting the highest pixel (0=absence, 1=presence). The annual accumulation area represented pixels that were covered at least once by the classified cyanobacteria accumulations in any of the images of that year, and was used as a measure of the extent of the accumulations.

As the AVHRR images were geometrically corrected and registered to a standard Albers equal area projection[15] with a 1 km^2 pixel size, the cumulative area in km^2 was simply calculated as the number of pixels different from zero.

We can expect that the total cumulative area is a "saturation" function which approaches a limit as the number of images per accumulation period increases. In stable weather conditions, the accumulations behave like passive contaminants, being advected by local currents and visible in the same locations for weeks. It is therefore expected that the detected total cumulative area will start to saturate as the number of images per bloom increases and each subsequent image will add less to the cumulative area as the pixels covered by the accumulations have already been marked on previous images.

We used this idea to construct an empirical correction factor for years with unequal amounts of data. To approximate the "saturation" function, we used the best sequence of 35 accumulation maps from the accumulation period of 1994. We simulated the process of accruing the total accumulation area from individual maps by adding the individual maps in random order. The individual simulations were then averaged and their standard deviations calculated.

The observed accumulation area was divided with the relative cumulative area corresponding to the respective number of images per accumulation period. Applying this correction func-

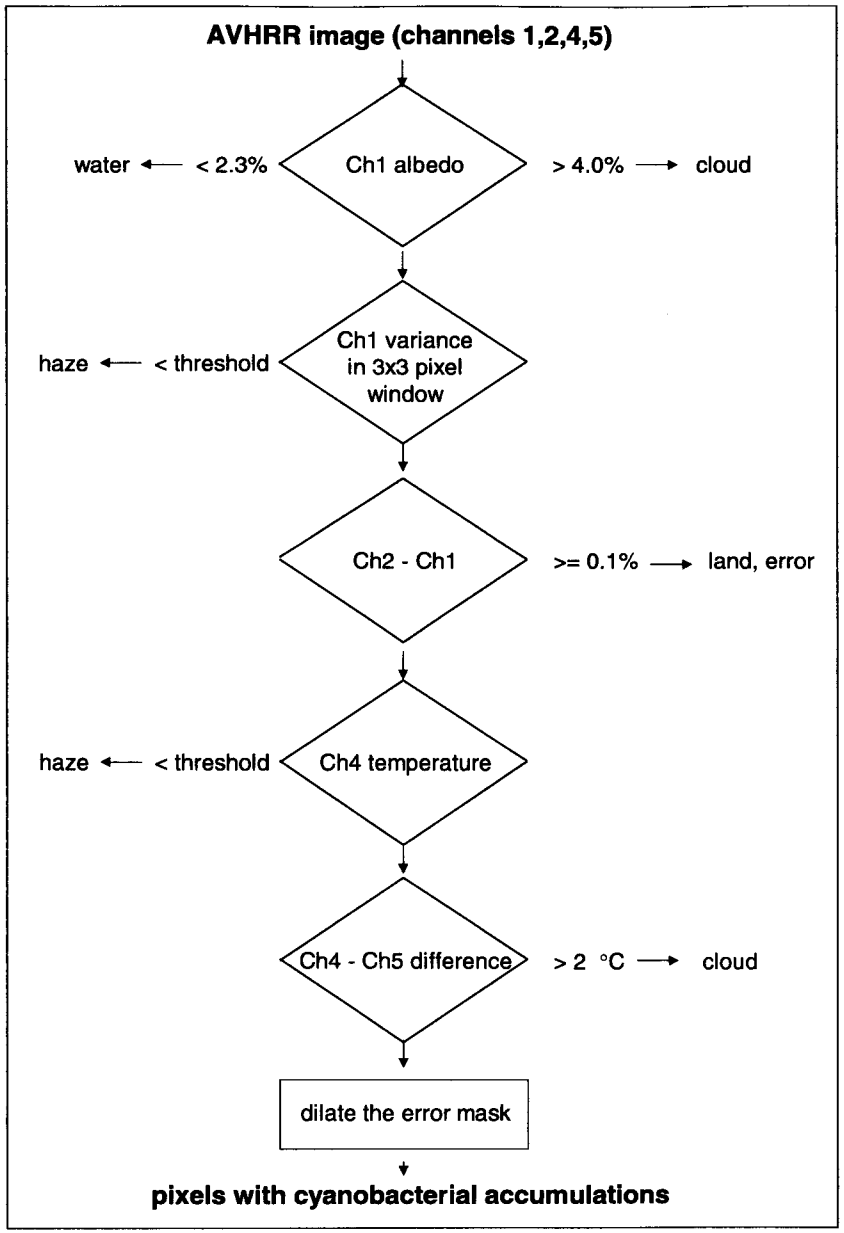

Fig. 3.2. Flowchart of the algorithm for detecting cyanobacteria accumulations from AVHRR channel 1-5 images.

tion to the observed cyanobacteria accumulations generated a corrected time series. The accumulation period was determined as the duration in days from the first until the last day when accumulations could be detected in any imagery (AVHRR, CZCS, TM and MSS).

Results

Observed Time Series

Surface accumulations of cyanobacteria blooms were detected in AVHRR imagery from late June to August of the year. Over the 13-year period from 1982 to 1994, the earliest was detected on June 30 (in 1990) and the latest on August 24 (in 1984). The remotely detectable cyanobacteria bloom over the Baltic Sea usually consists of several shorter periods in different regions (Fig. 3.3) which are interrupted by periods of high winds and rain (Fig. 3.4). The surface accumulations are quickly dispersed over the water column by wind induced mixing at wind speeds over 6-8 m s^{-1} (ref. 8)When suitable weather resumed, the accumulations sometimes reappeared in the same location but often appeared moving northwards. In some years the accumulations reappeared in the southernmost Baltic Sea during mid or late August (Fig. 3.3).

A time series of the cumulative area covered by cyanobacteria accumulations between 1982-1994 is shown in Figure 3.5. A period of low or missing blooms was evident from 1985 to 1988. No accumulations were detected in 1987 and 1988. Two conspicuous periods of increased cyanobacteria abundance were observed from 1982 to 1984 and from 1991 to 1994, with the greatest accumulation of over 100,000 km^2 recorded in 1994 (Fig. 3.6A). These two periods of increased accumulations coincided with periods of increased average sunshine duration (Fig. 3.7). When the correlative influence of the variable sunshine duration was excluded, the time series still showed a significant increase in the cyanobacteria accumulations in the 1990s.[7] For example, the 1993 cumulative area was disproportionately high considering the windy and cloudy weather and only average sunshine duration.

The detected total area of accumulations was, as noted previously, also a function of sampling frequency. Therefore, the time

series may be biased towards higher values in recent years when significantly improved sampling frequency (up to three satellite passes per day) existed.

Figure 3.8 shows the length of the accumulation period and the number of processed images available during that period. The bloom period actually starts before the accumulations appear at the surface and therefore remains undetected by imagery. Only images reasonably free of clouds, sun glint, and other disturbances were included in the analysis. While approximately 40 images were used per accumulation period in 1994, only 5 or less were available for the accumulation periods in the early 1980s. We can expect that the total areas for the latter period were underestimated and would be larger if more images were available.

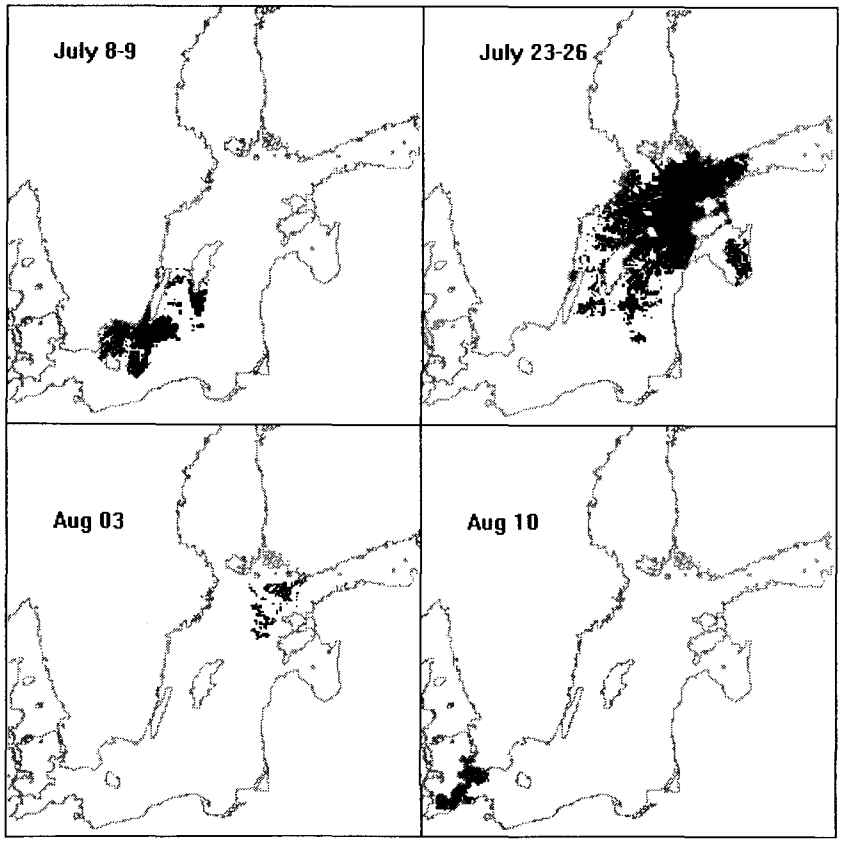

Fig. 3.3. Distribution of cyanobacteria accumulations in the Baltic Sea during four blooming events in 1992. The accumulations are marked as black dots on the contour map of the Baltic Sea.

Correction Factor Simulations

The simulated correction factor to correct for the bias due to sampling frequency showed the expected saturation shape (Fig. 3.9). In order to apply it to years with variable length of the accumulation period, the correction factor was normalized to the number of images per days of the accumulation period. Although this correction function is based on only one year's data and could behave differently for other patterns, we believe that it is a fair approximation to what occurs in the Baltic. We suspect that the saturation effect is diminished when accumulations appear in separate locations at different times during their seasonal occurrence.

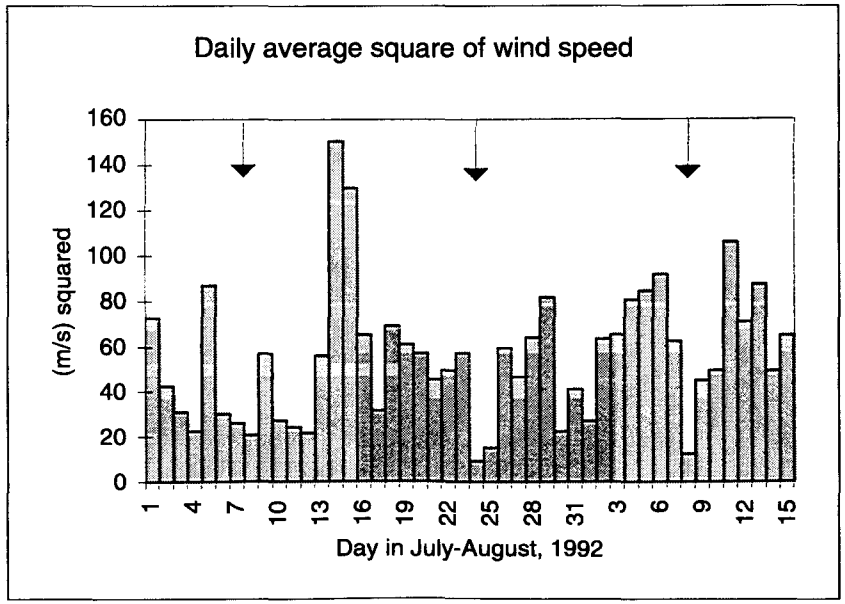

Fig. 3.4. Correspondence of cyanobacteria accumulations (indicated by arrows) to periods with low wind induced vertical mixing in July-August 1992.

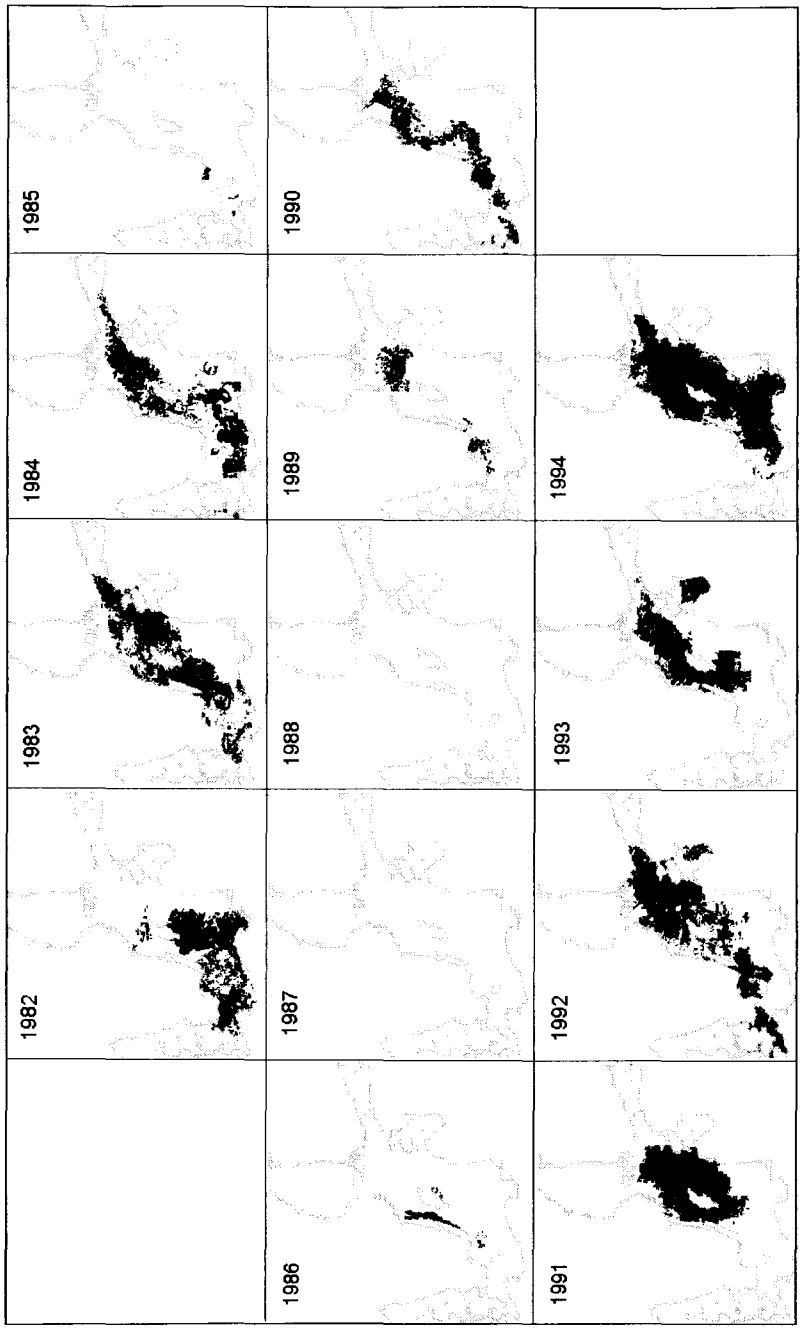

Fig. 3.5. Annual cumulative distributions of the cyanobacteria accumulations in the Baltic Sea between 1982-1994.

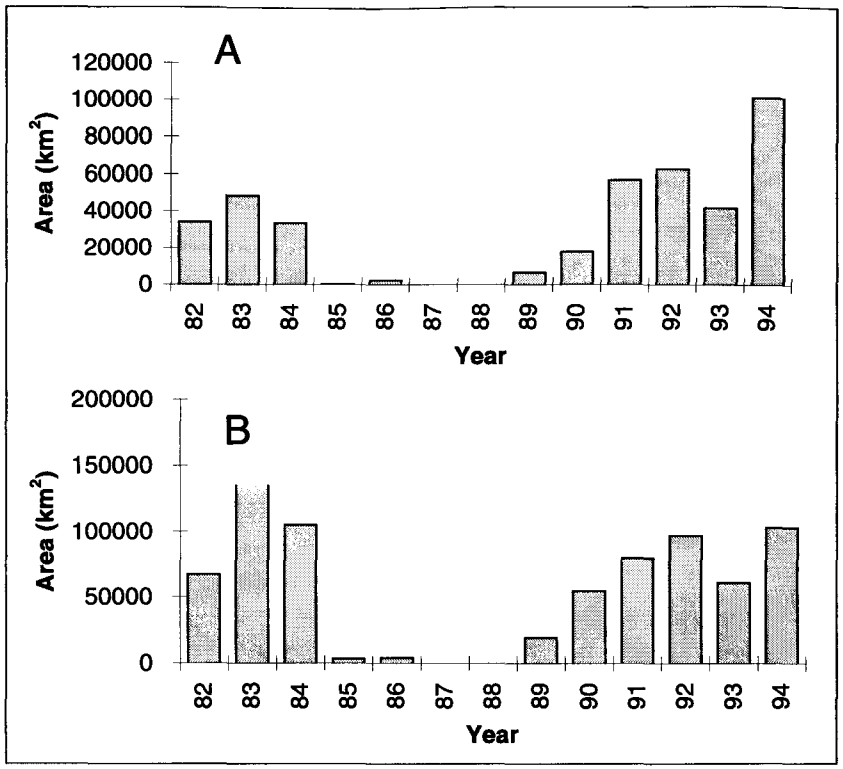

Fig. 3.6. Annual cumulative area covered by cyanobacteria accumulations in the Baltic Sea. The observed series (A) and the series corrected for the unequal number of images available per accumulation period (B).

Corrected Time Series

It is evident from the corrected time series that cyanobacteria maxima in the 1980s were comparable, if not higher, than the 1994 maximum of 100,000 km² (Fig. 3.6B). For example, the estimated total accumulation area in 1983 was about 150,000 km². Although there is no substitute for missing data, we believe that the corrected time series is a better approximation to reality than the observed series.

Discussion

Although frequent cloud cover over the Baltic Sea severely limits the amount of usable satellite data, cyanobacteria accumulations predominantly occur during periods of sunny and calm

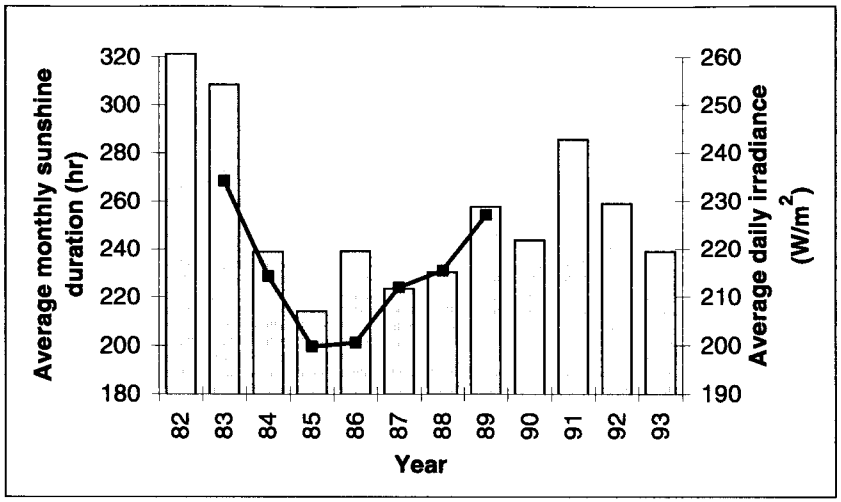

Fig. 3.7. Average monthly sunshine duration (bars) and daily surface irradiance (line) over the Baltic Sea in July and August from 1982 to 1993. The sunshine duration (left scale) is the average of measurements at two stations (Ölands Södra Udde and Visby) operated by the Swedish Meteorological and Hydrological Institute with pyrheliometers (time with irradiance >120 W m^{-2}). Average daily surface irradiance from 1983 to 1989 (right scale) has been compiled from data collected by the International Satellite Cloud Climatology Program[16] and was averaged over the Baltic Sea Proper area. Reprinted with permission from: Kahru M et al. Ambio 1994; 23:469-472. © 1994 Royal Swedish Academy of Sciences.

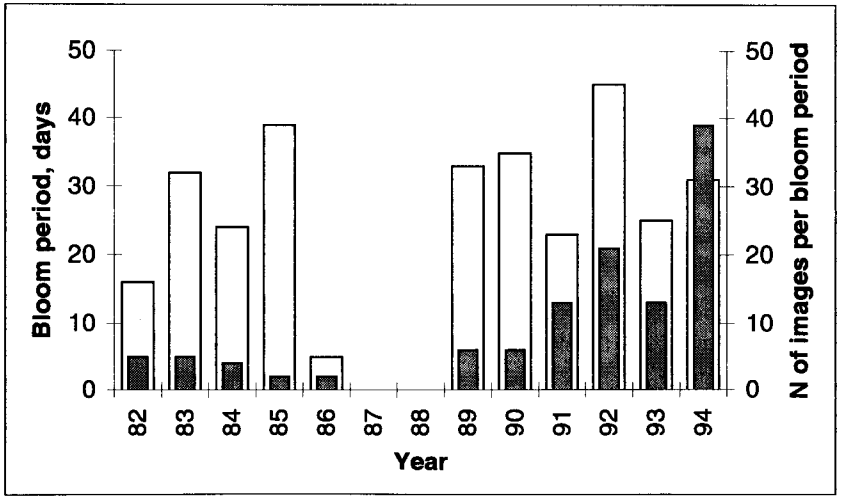

Fig. 3.8. The length of the accumulation period (open bar) and the number of processed images during the accumulation period (filled bar).

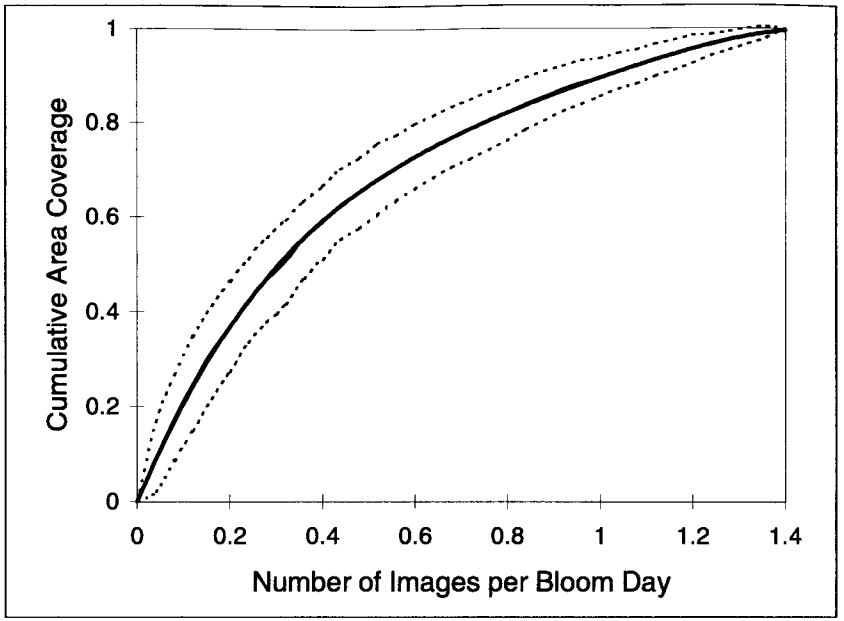

Fig. 3.9. Simulated cumulative area of cyanobacteria accumulations (± standard deviation) as a function of images per day of the bloom period. Reprinted with permission from: Kahru M, Rud O. Proc Third Conf on Remote Sensing for Marine and Coastal Environments 1995; 2:76-83. © 1995 Environmental Research Institute of Michigan.

weather when good imagery is available. This suggests that the bias towards clear weather periods is diminished when mapping the cyanobacteria accumulations with satellite imagery.

The detection of cyanobacteria surface accumulations in satellite imagery is probably the best tool available to map changes in the distribution of this ecologically important and environmentally sensitive phytoplankton group in the Baltic Sea. The empirical algorithm employed here is considered to be species-specific as the *Nodularia* "satellite signature" should not be confused with other species. An algorithm[17] used to detect *Trichodesmium*, another genus of cyanobacteria known to bloom in the surface layer of tropical oceans, in CZCS imagery was not applicable in the Baltic due to physically impossible negative values (as a result of high reflectivity at 550 nm). Also, the high reflectivity of cyanobacteria accumulations is similar to that of blooms of the coccolithophore *Emiliania huxleyi*, which is caused principally by the detached

coccoliths.[18-20] Yet the two groups should be distinguishable. The dense cyanobacteria accumulations floating at the very surface are reflective in the near-infrared (AVHRR band 2), whereas coccolithophore blooms should be essentially opaque at this wavelength because the coccoliths remain in the water column.

Furthermore, the AVHRR sensor may provide additional information about cyanobacteria blooms. The reflectance of the AVHRR band 2 relative to band 1 seems to be a function of the density, and potentially of physiological properties of cyanobacteria accumulations. Because of the variable reflectance of *Nodularia* accumulations in AVHRR band 2 the simple atmospheric correction used to enhance coccolithophore blooms[21,22] does not work with the cyanobacteria accumulations in the Baltic. However, the relative reflectances could yield useful information on these blooms if an optical model of *Nodularia* accumulations was available.

The real cyanobacteria bloom actually starts before the accumulations appear at the surface, and therefore remains undetected by AVHRR imagery. However, CZCS, OCTS and future ocean color satellites could probably detect it. Currently, the CZCS imagery still needs to be processed to produce results comparable to the AVHRR results, but it will eventually be merged with the time series produced from AVHRR data. The detected areas of cyanobacteria accumulations can only be regarded as the lower bounds of the actual total areas due to incomplete satellite sampling and frequent clouds obscuring the sea surface during satellite passes. There is, however, no doubt of the existence of two periods of increased cyanobacteria accumulations detected by the AVHRR from 1982 to 1984 and from 1991 to 1994. These periods coincide with periods of warm and sunny summers in the Baltic Sea area. The total area covered by surface-floating cyanobacteria increased to over 100,000 km^2 in 1994 and caught the attention of the general public and environmental planners. The question whether there has been any anthropogenic influence in the recent increase in cyanobacteria blooming remains unclear. A *Nodularia* bloom in its present extent was first described by shipborne observations a century ago.[23] Part, if not all, of the drastic increase in the satellite detected blooms the 1990s compared to early 1980s can be attributed to improved data coverage.

It is interesting to note that when the empirical correction factor compensating for the less frequent satellite coverage during the 1980s was applied, the corrected time series showed a cycle with two strong peaks and no overall increase. The cycle is similar to the El Niño—Southern Oscillation (ENSO) that is the dominant factor in multi-year climate variability in the tropics. With the exclusion of 1987, the cyanobacteria cycle bears close resemblance (with negative correlation) to the ENSO induced changes in vegetation in South Africa (P. Gondwe, personal communication). The correlation may be spurious, as ENSO effects in Europe are weak.[24] The existence of the cyanobacteria cycle with a period of approximately 10 years is apparent but no good explanations are available to account for it.

In addition to changes in the total area, the geographic locations of the accumulations have shown interesting features that are difficult to explain. For example, since 1992, the accumulations have reappeared in the western Gulf of Finland where they had been absent between 1985 and 1991. In the Bay of Gdansk, visible surface accumulations were missing between 1984 and 1993, and reappeared in 1994. In 1992 and 1993, massive visible accumulations were observed in the Gulf of Riga where they had not been observed before or after.

Due to dramatically increased nutrient loadings during recent decades,[5] the ecosystems of the Baltic Sea are under pressure to adjust in response to these changes. One possible adjustment to the increased P loading might be increased blooming of azotrophic cyanobacteria. The current satellite-based time series of *Nodularia* surface blooms does not, however, support an increase during the last two decades in the Baltic Sea.

Acknowledgments

I thank Ove Rud for help with satellite data processing, Prof. L. Wastenson for generous support while the author was a visiting scientist in Stockholm University, and Dr. Chris Brown for valuable recommendations on improving the manuscript.

References

1. Jansson B-O, Wilmot W, Wulff F. Coupling the subsystems—the Baltic Sea as a case study. In: Fasham MJR, ed. Flows of Energy and Materials in Marine Ecosystems. New York: Plenum, 1984:549-595.
2. Kahru M, Kaasik E, Leeben A. Annual cycle of particle size fractions and phytoplankton biomass in the northern Baltic proper. Mar Ecol Progr Ser 1991; 69:117-124.
3. Kononen K. Dynamics of the toxic cyanobacterial blooms in the Baltic Sea. Finn Mar Res 1992; 261:3-36.
4. Horstmann U. Eutrophication and mass occurrence of blue-green algae in the Baltic. Merentutkimuslait. Julk./Havsforskningsinst 1975; 239:83-90.
5. Larsson U, Elmgren R, Wulff F. Eutrophication and the Baltic Sea: causes and consequences. Ambio 1985; 14:9-14.
6. Håkansson B, Moberg M. The algal bloom in the Baltic during July and August 1991, as observed from the NOAA weather satellites. Int J Remote Sens 1994; 15:963-965.
7. Kahru M, Horstmann U, Rud O. Increased cyanobacterial blooming in the Baltic Sea detected by satellites: Natural fluctuation or ecosystem change? Ambio 1994; 23:469-472.
8. Kahru M, Leppänen J-M, Rud O. Cyanobacterial blooms cause heating of the sea surface. Mar Ecol Progr Ser 1993; 101:1-7.
9. Abbott MR, Brown OB, Evans RH et al. Ocean color in the 21st century: a strategy for a 20-year time series. NASA Tech Memo 104566, 1994; 17:1-20.
10. Acker JG. The heritage of SeaWiFS: a retrospective on the CZCS NIMBUS Experiment Team (NET) Program. NASA Tech Memo 104566, 1994; 21:1-43.
11. Kidwell KB. NOAA Polar Orbiter Data Users Guide (TIROS-N, NOAA-6, NOAA-7, NOAA-8, NOAA-9, NOAA-10, NOAA-11, NOAA-12, NOAA-14). Washington, DC: National Oceanic and Atmospheric Administration, 1995.
12. Kahru M, Rud O. Monitoring the decadal-scale variability of cyanobacteria blooms in the Baltic Sea by satellites. Proc Third Conference on Remote Sensing for Marine and Coastal Environments 1995; 2:76-83.
13. Agbu PA, James ME. The NOAA/NASA Pathfinder AVHRR Land Data Set User's Manual. Goddard Distributed Active Archive Center Publication, NASA, Goddard Space Flight Center, Greenbelt, MD, 1994.
14. Stumpf RP, Frayer ML. Use of AVHRR imagery to examine long-term trends in water clarity in coastal estuaries: Example in Florida Bay. In: Kahru M, Brown CW, ed. Monitoring Algal Blooms: New Techniques for Detecting Large-Scale Environmental Change. Austin: Landes Bioscience, 1997:1-23.

15. Baldwin DG, Emery WJ. A systematized approach to AVHRR navigation. Ann Glaciol 1993; 17:414-420.
16. Bishop J, Rossow W. Spatial and temporal variability of global surface solar irradiance. J Geophys Res Atmos 1991; 96:16839-16858.
17. Subramaniam A, Carpenter EJ. An empirically derived protocol for the detection of blooms of the marine cyanobacterium *Trichodesmium* using CZCS imagery. Int J Remote Sens 1994; 15:1559-1569.
18. Ackleson SG, Balch WM, Holligan PM. AVHRR observations of a Gulf of Maine coccolithophore bloom. Photogramm Eng Remote Sensing 1989; 55:473-474.
19. Ackleson SG, Holligan PM. Response of water-leaving radiance to particulate calcite and chlorophyll *a* concentrations: A model for the Gulf of Maine coccolithophore blooms. J Geophys Res Oceans 1994; 99:7483-7499.
20. Brown CW, Yoder JA. Coccolithophorid blooms in the global ocean. J Geophys Res Oceans 1994; 99:7467-7482.
21. Groom SB, Holligan PM. Remote sensing of coccolithophore blooms. Adv Space Res 1987; 7:73-78.
22. Gower JFR. Red tide monitoring using AVHRR HRPT imagery from a local receiver. Remote Sens Environ 1994; 48:309-318.
23. Apstein C. Das Plankton der Ostsee (Holsatia Expedition 1901). Abhandlungen d Seefischerievereins 1902; 7:103-129.
24. Fraedrich K. An ENSO Impact on Europe? A Review. Tellus (A) 1994; 46:541.